1 **A GENERALISED RANDOM ENCOUNTER MODEL FOR ESTIMATING**
2 **ANIMAL DENSITY WITH REMOTE SENSOR DATA**

3 **Running title: A generalised random encounter model for animals.**

4 **Word count:**

5 **Authors:**

6 Tim C.D. Lucas[1,2,3], Elizabeth A. Moorcroft[1,4,5], Robin Freeman[5], Marcus J. Rowcliffe[5],

7 Kate E. Jones[2,5]

8 **Addresses:**

9 1 CoMPLEX, University College London, Physics Building, Gower Street, Lon-

10 don, WC1E 6BT, UK

11 2 Centre for Biodiversity and Environment Research, Department of Genetics,

12 Evolution and Environment, University College London, Gower Street, London,

13 WC1E 6BT, UK

14 3 Department of Statistical Science, University College London, Gower Street,

15 London, WC1E 6BT, UK

16 4 Department of Computer Science, University College London, Gower Street,

17 London, WC1E 6BT, UK

18 5 Institute of Zoology, Zoological Society of London, Regents Park, London, NW1

19 4RY, UK

20 **Corresponding authors:**

21 Kate E. Jones,

22 Centre for Biodiversity and Environment Research,

23 Department of Genetics, Evolution and Environment,

24 University College London,

25 Gower Street,

26 London,

27 WC1E 6BT,

28 UK

29 kate.e.jones@ucl.ac.uk

30

31   Marcus J. Rowcliffe,

32 Institute of Zoology,

33 Zoological Society of London,

34 Regents Park,

35 London,

36 NW1 4RY,

37 UK

38 marcus.rowcliffe@ioz.ac.uk

ABSTRACT

1: Wildlife monitoring technology has advanced rapidly and the use of remote sensors such as camera traps, and acoustic detectors is becoming common in both the terrestrial and marine environments. Current methods to estimate abundance or density require individual recognition of animals or knowing the distance of the animal from the sensor, which is often difficult. A method without these requirements, the random encounter model (REM), has been successfully applied to estimate animal densities from count data generated from camera traps. However, count data from acoustic detectors do not fit the assumptions of the REM due to the directionality of animal signals.

2: We developed a generalised REM (gREM), to estimate absolute animal density from count data from both camera traps and acoustic detectors. We derived the gREM for different combinations of sensor detection widths and animal signal widths (a measure of directionality). We tested the accuracy and precision of this model using simulations of different combinations of sensor detection widths and animal signal widths, number of captures, and models of animal movement.

3: We find that the gREM produces accurate estimates of absolute animal density for all combinations of sensor detection widths and animal signal widths. However, larger sensor detection and animal signal widths were found to be more precise. While the model is accurate for all capture efforts tested, the precision of the estimate increases with the number of captures. We found no effect of different animal movement models tested on the accuracy and precision of the gREM.

4: We conclude that the gREM provides an effective method to estimate absolute animal densities from remote sensor count data over a range of sensor and animal signal widths. The gREM is applicable for count data obtained in both marine and terrestrial environments, visually or acoustically (e.g., big cats, sharks, birds, bats and cetaceans). As sensors such as camera traps and acoustic detectors become more ubiquitous, the gREM will be increasingly useful for monitoring unmarked animal populations across broad spatial, temporal and taxonomic scales.

INTRODUCTION

Animal population density is one of the fundamental measures needed in ecology and conservation. The density of a population has important implications for a range of issues such as sensitivity to stochastic fluctuations (Richter-Dyn & Goel, 1972; Wright & Hubbell, 1983) and risk of extinction (Purvis *et al.*, 2000). Monitoring animal population changes in response to anthropogenic pressure is becoming increasingly important as humans modify habitats and change climates as never before (Everatt *et al.*, 2014). Sensor technology, such as camera traps (Rowcliffe & Carbone, 2008; Karanth, 1995) and acoustic detectors (O'Farrell & Gannon, 1999; Clark, 1995; Acevedo & Villanueva-Rivera, 2006) are becoming increasingly used to monitor changes in animal populations (Rowcliffe & Carbone, 2008; Kessel *et al.*, 2014), as they are efficient, relativity cheap and non-invasive (Cutler & Swann, 1999), allowing for surveys over large areas and long periods. However, the problem of converting sampled count data to estimates of density remains as efforts must be made to account for detectability of the animals (Anderson, 2001).

Methods do already exist for estimating animal density if the distance between the animal and the sensor can be estimated (e.g., capture-mark recapture methods (Karanth, 1995) and distance sampling (Harris *et al.*, 2013)). However, these methods often require additional information that may not be available. For example, capture-mark-recapture methods (Karanth, 1995; Trolle & Kéry, 2003; Soisalo & Cavalcanti, 2006; Trolle *et al.*, 2007) require recognition of individuals; distance methods require a distance estimation of how far away individuals are from the sensor (Barlow & Taylor, 2005; Marques *et al.*, 2011). The development of the random encounter model (REM) (a modification of a gas model) enabled animal densities to be estimated from unmarked individuals of a known speed, and sensor detection parameters (Rowcliffe *et al.*, 2008). The REM method has been successfully applied to estimate animal densities from camera trap surveys (Manzo *et al.*, 2012; Zero *et al.*, 2013). However, extending the REM method to other types of sensors (for example acoustic detectors) is more problematic, because the original

99   derivation assumes a relatively narrow sensor width (up to $\pi/2$ radians) and that

100   the animal is equally detectable irrespective of its heading (Rowcliffe *et al.*, 2008).

101   Whilst these restrictions are not problematic for most camera trap makes (e.g.

102   Reconyx, Cuddeback), the REM could not be used to estimate densities from cam-

103   era traps with a wider sensor width (e.g. canopy monitoring with fish eye lens

104   (Brusa & Bunker, 2014)). Additionally, the REM method would not be useful in

105   estimating densities from acoustic survey data as the acoustic detector angles are

106   often wider than $\pi/2$ radians. Acoustic detectors are designed for a range of di-

107   verse tasks and environments (Kessel *et al.*, 2014), which will naturally lead to a

108   wide range of sensor detection widths and detection distances. In addition to this,

109   calls emitted by many animals are directional (Blumstein *et al.*, 2011) (breaking the

110   assumption of the REM method).

111   There has been a sharp rise in interest around passive acoustic detectors in re-

112   cent years, with a 10 fold increase in publications in the decade between 2000 and

113   2010 (Kessel *et al.*, 2014). Acoustic monitoring is being developed to study many

114   aspects of ecology, including the interactions of animals and their environments

115   (Blumstein *et al.*, 2011; Rogers *et al.*, 2013), the presence and relative abundances of

116   species (Marcoux *et al.*, 2011), and biodiversity of an area (Depraetere *et al.*, 2012).

117   Acoustic data suffers from many of the problems associated with data from

118   camera trap surveys in that individuals are often unmarked so capture-make-

119   recapture methods cannot be used to estimate densities. In some cases the dis-

120   tance between the animal and the sensor is known, for example when an array of

121   sensors and the position of the animal is estimated by triangulation (Lewis *et al.*,

122   2007). In these situations distance-sampling methods can be applied, a method

123   typically used for marine mammals (Rogers *et al.*, 2013). However, in many cases

124   distance estimation is not possible, for example when single sensors are deployed,

125   a situation typical in the majority of terrestrial acoustic surveys (Elphick, 2008;

126   Buckland *et al.*, 2008). In these cases, only relative measures of local abundance

127   can be calculated, and not absolute densities. This means that comparison of

128   populations between species and sites is problematic without assuming equal de-

129   tectability (Schmidt, 2003). Equality detectability is unlikely because of differences

130   in environmental conditions, sensor type, habitats, species biology.

In this study we create a generalised REM (gREM), as an extension to the camera trap model of (Rowcliffe *et al.*, 2008), to estimate absolute density from count data from acoustic detectors, or camera traps, where the sensor width can vary from 0 to 2π radians, and the signal given off from the animal can be directional. We assessed the accuracy and precision of the gREM within a simulated environment, by varying the sensor detection widths, animal signal widths, number of captures and models of animal movement. We use the simulation results to recommend best survey practice for estimating animal densities from remote sensors.

<div align="center">METHODS</div>

Analytical Model. The REM presented by (Rowcliffe *et al.*, 2008) adapts the gas model to model count data from camera trap surveys. The REM is derived assuming a stationary sensor with a detection width less than $\pi/2$ radians. However, in order to apply this approach more generally, and in particular to acoustic detectors, we need both to relax the constraint on sensor detection width, and allow for animals with directional signals. Consequently, we derive the gREM for any detection width, θ, between 0 and 2π with a detection distance r giving a circular sector within which animals can be captured (the detection zone)(Figure 1). Additionally, we model the animal as having an associated signal width α between 0 and 2π(Figure 1, see Appendix S1 for a list of symbols). We start deriving the gREM with the simplest situation, the gas model where $\theta = 2\pi$ and $\alpha = 2\pi$.

Gas Model. Following Yapp (1956), we derive the gas model where sensors can capture animals in any direction and animal's signal is detectable from any direction($\theta = 2\pi$ and $\alpha = 2\pi$). We assume that animals are in a homogeneous environment, and move in straight lines of random direction with velocity v. We allow that our stationary sensor can capture animals at a detection distance r and that if an animal moves within this detection zone they are captured with a probability of one, while animals outside the zone are never captured.

In order to derive animal density, we need to consider relative velocity from the reference frame of the animals. Conceptually, this requires us to imagine that all animals are stationary and randomly distributed in space, while the sensor moves with velocity v. If we calculate the area covered by the sensor during the

<div align="center">6</div>

162 survey period we can estimate the number of animals the sensor should capture.

163 As a circle moving across a plane, the area covered by the sensor per unit time is

164 $2rv$. The number of expected captures, z, for a survey period of t, with an animal

165 density of D is $z = 2rvtD$. To estimate the density, we rearrange to get $D = z/2rvt$.

166 *gREM derivations for different detection and signal widths.* Different combinations of

167 θ and α would be expected to occur (e.g., sensors have different detection widths

168 and animals have different signal widths). For different combinations θ and α, the

169 area covered per unit time is no longer given by $2rv$. Instead of the size of the

170 sensor detection zone having a diameter of $2r$, the size changes with the approach

171 angle between the sensor and the animal. For any given signal width and detec-

172 tor width and depending on the angle that the animal approaches the sensor, the

173 width of the area within which an animal can be detected is called the profile, p.

174 The size of the profile (averaged across all approach angles) is defined as the aver-

175 age profile $\bar{p}$. However, different combinations of θ and α need different equations

176 to calculate $\bar{p}$.

177 We have identified the parameter space for the combinations of θ and α for

178 which the derivation of the equations are the same (defined as sub-models in the

179 gREM) (Figure 2). For example, the gas model becomes the simplest gREM sub-

180 model (upper right in (Figure 2) and the REM from (Rowcliffe *et al.*, 2008) is an-

181 other gREM sub-model where $\theta < \pi/2$ and $\alpha = 2\pi$. We derive one gREM sub-model

182 SE2 as an example below (where $4\pi - 2\alpha < \theta < 2\pi,\ 0 < \alpha < \pi$) (see Appendix S2 for

183 other gREM sub-models).

184 *Example derivation of SE2.* In order to calculate $\bar{p}$, we have to integrate over the

185 focal angle, x_1 (Figure 3a). This is the angle taken from the centre line of the sensor.

186 Other focal angles are possible (x_2, x_3, x_4) and are used in other gREM sub-models

187 (see Appendix S2). As the size of the profile depends on the approach angle, we

188 present the derivation across all approach angles. When the sensor is directly

189 approaching the animal $x_1 = \pi/2$.

190 Starting from $x_1 = \pi/2$ until $\theta/2 + \pi/2 - \alpha/2$, the size of the profile is $2r \sin \alpha/2$

191 (Figure 3b). During this first interval, the size of α limits the width of the profile.

192 When the animal reaches $x_1 = \theta/2 + \pi/2 - \alpha/2$ (Figure 3c), the size of the profile is

7

193 $r\sin(\alpha/2) + r\cos(x_1 - \theta/2)$ and the size of $\theta/$ and α both limit the width of the profile

194 (Figure 3c). Finally, at $x_1 = 5\pi/2 - \theta/2 - \alpha/2$ until $x_1 = 3\pi/2$, the width of the profile

195 is again $2r\sin\alpha/2$ (Figure 3d) and the size of α again limits the width of the profile.

196   The profile width p for π radians of rotation (from directly towards the sensor

197 to directly behind the sensor) is completely characterised by the three intervals

198 (Figure 3b–3d). Average profile width $\bar{p}$ is calculated by integrating these profiles

199 over their appropriate intervals of x_1 and dividing by π which gives

$$\bar{p} = \frac{1}{\pi}\left(\int_{\frac{\pi}{2}}^{\frac{\pi}{2}+\frac{\theta}{2}-\frac{\alpha}{2}} 2r\sin\frac{\alpha}{2}\,dx_1 + \int_{\frac{\pi}{2}+\frac{\theta}{2}-\frac{\alpha}{2}}^{\frac{5\pi}{2}-\frac{\theta}{2}-\frac{\alpha}{2}} r\sin\frac{\alpha}{2} + r\cos\left(x_1 - \frac{\theta}{2}\right)\,dx_1 + \int_{\frac{5\pi}{2}-\frac{\theta}{2}-\frac{\alpha}{2}}^{\frac{3\pi}{2}} 2r\sin\frac{\alpha}{2}\,dx_1 \right)$$

<div align="right">eqn 1</div>

$$= \frac{r}{\pi}\left(\theta\sin\frac{\alpha}{2} - \cos\frac{\alpha}{2} + \cos\left(\frac{\alpha}{2} + \theta\right) \right) \qquad\qquad \text{eqn 2}$$

200   We then, as with the gas model, use this expression to calculate density

201 $$D = z/vt\bar{p}. \qquad\qquad \text{eqn 3}$$

202   Rather than having one equation that describes $\bar{p}$ globally, the gREM must be

203 split into submodels due to discontiunous changes in p as α and β change. These

204 discontinuities can occur for a number of reasons such as a profile switching be-

205 tween being limited by α and θ, the difference between very small profiles and

206 profiles of size zero and the fact that the width of a sector stops increasing once

207 the central angle reaches π radians (i.e., a semi circle is just as wide as a full circle.)

208   As a visual example, if α is small, there is an interval between Fig. 3c and 3d

209 where the 'blind spot' would prevent animals being detected at all giving $p = 0$.

210 This would require an extra integral in our equation as simply putting our small

211 value of α into eqn 1 would not give us this integral of $p = 0$.

212   gREM submodel specifications were done by hand, and the integration was

213 done using SymPy (SymPy Development Team, 2014) in Python (Appendix S3).

214 The gREM submodels were checked by confirming that: (1) submodels adjacent

215 in parameter space were equal at the boundary between them; (2) submodels that

216 border $\alpha = 0$ had $p = 0$ when $\alpha = 0$; (3) average profile widths $\bar{p}$ were between 0

²¹⁷ and 2*r* and; (4) each integral, divided by the range of angles that it was integrated

²¹⁸ over, was between 0 and 2*r*. The scripts for these tests are included in Appendix

²¹⁹ S3 and the R (R Development Core Team, 2010) implementation of the gREM is

²²⁰ given in Appendix S4.

²²¹ **Simulation Model.** We tested the accuracy and precision of the gREM by devel-

²²² oping a spatially explicit simulation of the interaction of sensors and animals using

²²³ different combinations of sensor detection widths, animal signal widths, number

²²⁴ of captures, and models of animal movement. 100 simulations were run where

²²⁵ each consisted of a 7.5 km by 7.5 km square (with periodic boundaries). A station-

²²⁶ ary sensor of radius *r* was set up in the exact centre of each simulation, covering

²²⁷ 7 sensor detection widths θ between 0 and 2π ($2/9\pi$, $4/9\pi$, $6/9\pi$, $8/9\pi$, $10/9\pi$, $14/9\pi$,

²²⁸ 2π). Each simulation was populated with a density of 70 animals km^{-2}, calculated

²²⁹ from the equation in Damuth (1981) as the expected density of mammals of weigh-

²³⁰ ing 1 g. This density therefore represents the highest likely density of indivudals,

²³¹ given that the smallest mammal is around 2 g (Jones *et al.*, 2009). A total of 3937

²³² individuals per simulation were created which were placed randomly at the start

²³³ of the simulation. Individuals were assigned 11 signal detection widths α between

²³⁴ 0 and π ($1/11\pi$, $2/11\pi$, $3/11\pi$, $4/11\pi$, $5/11\pi$, $6/11\pi$, $7/11\pi$, $8/11\pi$, $9/11\pi$, $10/11\pi$, π).

²³⁵ Each simulation lasted for *N* steps (14400) of duration *T* (15 minutes) giving a

²³⁶ total duration of 150 days. The individuals moved within each step with a distance

²³⁷ *d*, with an average speed, *v*. *d*, was sampled from a normal distribution with

²³⁸ mean distance, $\mu_d = vT$, and standard deviation $\sigma_d = vT/10$. An average speed,

²³⁹ $v = 40$ km days^{-1}, was chosen as this represents the largest day range of terrestrial

²⁴⁰ animals (Carbone *et al.*, 2005), and represents the upper limit of realistic speeds.

²⁴¹ At the end step, individuals were allowed to either remain stationary for a time

²⁴² step (with a given probability, *S*), change direction (with a maximum angle, *A*)

²⁴³ between 0 and π. This resulted in 7 different movement models where: (1) simple

²⁴⁴ movement, where *S* and $A = 0$; (2) stop-start movement, where (i) $S = 0.25$, $A = 0$,

²⁴⁵ (ii) $S = 0.5$, $A = 0$, (iii) $S = 0.75$, $A = 0$; (3) random walk movement, where (i) $S = $

²⁴⁶ 0, $A = \pi/3$, (ii) $S = 0$, $A = 2\pi/3$, iii) $S = 0$, $A = \pi$. Individuals were counted as they

²⁴⁷ moved in and out of the detection zone of the sensor per simulation.

248   We calculated the estimated animal density from the gREM by summing the

249 number of captures per simulation and inputting these values into the correct

250 gREM submodel. gREM accuracy was determined by comparing the density in

251 the simulation with the estimated density. High accuracy is indicated by the mean

252 difference between the estimated and actual values not being significantly differ-

253 ent from zero (Wilcoxon signed-rank test). gREM precision was determined by

254 the standard deviation of estimated densities. We used this method to compare

255 the accuracy and precision of all the gREM submodels. As these submodels are

256 derived for different combinations of α and θ, the accuracy and precision of the

257 submodels was used to determine the impact of different values of α and θ.

258   The influence of the number of captures and animal movement models on accu-

259 racy and precision was investigated using 4 different gREM submodels represen-

260 tative of the range α and θ values (submodels NW1, SW1, NE1, and SE3, Figure 2).

261 Using these four submodels, we calculated how long the simulation needed to

262 run to generate a range of different capture numbers (from 10 to 100 captures in

263 10 unit intervals), and estimated animal density. These estimated densities were

264 compared to the real density to assess the impact on the accuracy and precision

265 on the gREM of different simulation lengths. We also used these four submodels

266 to compare the accuracy and precision of a simple movement model, to stop-start

267 movement models and random walk movement models. The gREM assumes that

268 individuals move continuously with straight-line movement (simple movement

269 model) and we therefore assessed the impact of breaking the gREM assumptions.

270   RESULTS

271 **Analytical model.** The equation for $\bar{p}$ has been newly derived for each submodel

272 in the gREM, except for the gas model and REM which have been calculated pre-

273 viously. However, many models, although derived separately, have the same ex-

274 pression for $\bar{p}$. Figure 4 shows the expression for $\bar{p}$ in each case. The general equa-

275 tion for density, using the correct expression for $\bar{p}$ is then substituted into eqn 3.

276 Although more thorough checks are performed in Appendix S3, it can be seen that

277 all adjacent expressions in Figure 4 are equal when expressions for the boundaries

278 between them are substituted in.

Simulation model.

gREM submodels. All gREM submodels showed a high accuracy, i.e., the mean difference between the estimated and actual values was not significantly different from zero across all models, corrected for multiple tests (all gREM sub models Wilcoxon signed-rank test, p >0.002)(Figure 5). However, the precision of the submodels do vary, where the gas model is the most precise and the SW7 sub model the least precise, having the smallest and the largest interquartile range, respectively (Figure 5). The standard deviation of the error between the estimated and true densities is strongly related to both the sensor and signal widths (Figure 6), such that larger widths have lower standard deviations (greater precision). However, even smaller sensor and signal widths have a relativity high level of precision.

Number of captures. Within the four gREM submodels tested (NW1, SW1, SE3, NE1), the accuracy was not affected by the number of captures, where the mean difference between the estimated and actual values was not significantly different from zero across all capture rates, corrected for multiple tests (all gREM sub models Wilcoxon signed-rank test, p >0.008)(Figure 7). However, the precision was dependent on the number of captures across all four of the gREM submodels, where precision increases as number of captures increases (Figure 7). For all gREM submodels, the the coefficient of variation falls to 10% at 100 captures.

Movement models. Within the four gREM submodels tested (NW1, SW1, SE3, NE1), neither the accuracy or precision was affected by the amount of time spent stationary. The mean difference between the estimated and actual values was not significantly different from zero for each category of stationary time (0, 0.25, 0.5 and 0.75), corrected for multiple tests (all gREM sub models Wilcoxon signed-rank test, p >0.12)(Figure 8a). Altering the maximum change in direction in each step (0, pi/3, 2pi/3, and pi) did not affect the accuracy or precision of the four gREM submodels tested (all gREM sub models Wilcoxon signed-rank test, p >0.05)(Figure 8b).

11

₃₀₈ DISCUSSION

₃₀₉ We have developed the gREM such that it can be used to estimate density from

₃₁₀ acoustic sensors and camera traps. This has entailed a generalisation of the gas

₃₁₁ model and the REM in Rowcliffe *et al.* (2008) to be applicable to any combination

₃₁₂ of sensor width and signal directionality. We have used simulations to show, as a

₃₁₃ proof of principle, that these models are accurate and precise. The precision of the

₃₁₄ gREM was found to be dependent on the width of the sensor and the call, and the

₃₁₅ number of captures.

₃₁₆ **Analytical model.** The gREM was derived for different combinations of α and θ

₃₁₇ resulting in 25 different submodels, the expression for $\bar{p}$ are equal for many of

₃₁₈ these submodels resulting in eight different equations including the previously

₃₁₉ derived gas model and REM. These submodels were tested for consistency with

₃₂₀ adjacent expressions being equal at their boundaries. These new submodels will

₃₂₁ allow researchers to evaluate the absolute density of animals that have previously

₃₂₂ been difficult to study, such as bats (Clement & Castleberry, 2013), with noninva-

₃₂₃ sive methods such as remote sensors. The gREM allows the data from acoustic

₃₂₄ detectors to be used where an animal has a directional calls, this could be used

₃₂₅ for a range of animals including songbirds (Blumstein *et al.*, 2011), and dolphins

₃₂₆ (Lammers & Au, 2003).

₃₂₇ There are a number of possible extensions to the gREM which could be devel-

₃₂₈ oped in the future. The original gas model was formulated for the case where both

₃₂₉ subjects, either animal and detector, or animal and animal, are moving (Hutchin-

₃₃₀ son & Waser, 2007). Indeed any of the models with animals that are equally de-

₃₃₁ tectable in all directions ($\alpha = 2\pi$) can be trivially expanded for moving by substi-

₃₃₂ tuting the sum of the average animal velocity and the sensor velocity for *v* as used

₃₃₃ here. However, when the animal has a directional call, as seen in both terrestrial

₃₃₄ and aquatic environments (Lammers & Au, 2003; Blumstein *et al.*, 2011), the ex-

₃₃₅ tension becomes less simple. The approach would be to calculate again the mean

₃₃₆ profile width. However, for each angle of approach, one would have to average

₃₃₇ the profile width for an animal facing in any direction (i.e. not necessarily moving

₃₃₈ towards the sensor) weighted by the relative velocity of that direction. There are

339 a number of situations where a moving detector and animal could occur and as

340 such may be advantage to have a method of estimating densities from the data

341 collected, e.g. an acoustic detector towed from a boat when studying porpoises

342 (Kimura *et al.*, 2014) or surveying bats from a moving car (Ahlen & Baagøe, 1999).

343 An interesting but unstudied problem is edge effects caused by trigger delays

344 (the delay between sensing an animal and attempting to record the encounter)

345 (Rovero *et al.*, 2013) and time expansion acoustic detectors which repeatedly turn

346 on an off during sampling (Ahlen & Baagøe, 1999). Both of these have potential bi-

347 ases as animals can move through the detection zone without being detected. The

348 models herein are formulated assuming constant surveillance and so the error cre-

349 ated by switching the camera on and off quickly becomes negligible if the sensor

350 is on for extended periods of time. For example, if it takes longer for the record-

351 ing device to be switched on than the length of some animal calls there could be a

352 systematic underestimation of density.

353 **Accuracy and Precision.** Based on our simulations we believe that the gREM has

354 the potential to produce accurate estimates for many different species, using ei-

355 ther camera traps or acoustic detectors. However the precision of the gREM dif-

356 fered between submodels. For example, when the sensor and signal width were

357 smaller then the precision of the model was reduced, so when choosing a sensor

358 for use in a gREM study the detection width should be maximised, and if the study

359 species has a narrow signal directionality other aspects of the study protocol, such

360 as length of the survey, should be used to compensate.

361 The precision of the gREM is greatly affected by the number of captures that are

362 collected, the coefficient of variation falls dramatically between 10 and 60 captures

363 and then after this continues to slowly reduce. At 100 captures the submodels

364 reach 10% coefficient of variation, considered to a very good level of precision

365 (Thomas & Marques, 2012). Many current studies to not reach this level of pre-

366 cision, with most studies reporting coefficient of variations greater than the 10%

367 level (O'Brien *et al.*, 2003; Proctor *et al.*, 2010; Foster & Harmsen, 2012). The length

368 of surveys in the field will need to be adjusted so that enough data is collected to

369 reach this level of precision, populations of fast moving animals or populations

with large densities will require less survey effort than those with slow moving or low densities.

The gREM was both accurate and precise for all the movement models we tested against, stop-start movement and correlated random walks. However these movement models are still simple representations of true animal movement which often consist of multiple be dependent on multiple factors such as behavioural state and and existence of home ranges (Smouse *et al.*, 2010). The accuracy of the gREM may be affected by the interaction between the movement model and the size of the detection radius. We have studied a relatively long step length compared to the size of the detection radius, and therefore the chance of catching the same animal multiple times within a short space of time was reduced and there is little affect on the precision of the model (Figure 8b). However if the ratio of step length to detection radius was smaller then this may decrease the precision of the model, however this should not decrease its accuracy.

Although we have used simulations to validate the gREM submodels, much more robust testing is needed. Although difficult, proper field test validation would be required before the models could be fully trusted. The REM (Rowcliffe *et al.*, 2008) has already been field tested, and both Rowcliffe *et al.* (2008) and Zero *et al.* (2013) both found that the REM was an effective manner of estimating animal densities (Rowcliffe *et al.*, 2008; Zero *et al.*, 2013). In some taxa gold standard methods of estimating animal density exist, such as capture mark recapture (Sollmann *et al.*, 2013). Where these gold standard exist or true numbers are known, a simultaneous gREM study could be completed to test the accuracy under field conditions, similar to the tests that Rowcliffe *et al.* (2008) completed with the REM. An easier way to continue to evaluate the models is to run more extensive simulations which break the assumptions of the analytical models. The main element that cannot be analytically treated is the complex movement of real animals. Therefore testing these methods against true animal traces, or more complex movement models would be required.

Within the simulation we have assumed an equal density across the entire world, however in a field environment the situation would be much more complex, with additional variation coming from local changes in density between camera sites.

14

402 We allowed the sensor to be stationary and on all the time, negating the triggering,

403 and time expansion issues that could exist in real life. In the simulation we ran the

404 speed of the animal as $40 \, \mathrm{km \, days^{-1}}$, the largest day range of terrestrial animals

405 (Carbone *et al.*, 2005), other speed values should not alter the accuracy or the pre-

406 cision of the gREM. We also assume perfect knowledge of the average speed of an

407 animal and size of the detection zone, and instant triggering of the camera. All of

408 which may lead to possible bias or a decrease in precision.

409 **Implications for conservation.** The gREM is therefore available for the estimation

410 of density of a number of taxa where no, or few, accurate methods currently exist

411 to measure absolute animal density (Thomas & Marques, 2012). The species that

412 can now be studied may be of importance to conservation, for example current

413 methods of density estimation for the threatened Francisana dolphin may result

414 in underestimation of numbers (Crespo *et al.*, 2010). This new methods may be im-

415 portant for the study of zoonotic diseases, for example estimating bat population

416 size, which have previously been difficult to study(Robinson & Stebbings, 1997),

417 but are important reservoir of infectious disease that effect humans, livestock and

418 wildlife (Calisher *et al.*, 2006). In addition, the gREM will make it possible to mea-

419 sure the density of animals may be useful in ecosystem services, such as studying

420 the levels of songbirds which are known to have a positive influence on pest con-

421 trol in coffee production (Jirinec *et al.*, 2011). The gREM is suitable for any species

422 that would be consistently recorded at least once when within range of a detector,

423 such as bats (Kunz *et al.*, 2009), songbirds (Buckland & Handel, 2006), whales (Mar-

424 ques *et al.*, 2009) or forest primates (Hassel-Finnegan *et al.*, 2008). Within increasing

425 technological capabilities, this list of species is likely to increase dramatically.

426 Importantly the of camera trapping and acoustically recording that the gREM

427 use are noninvasive and do not require human marking (Jewell, 2013) or natu-

428 rally identifying marks (as required for mark-recapture models). This makes them

429 suitable for large, continuous monitoring projects with limited human resources

430 (Kelly *et al.*, 2012). It also makes them suitable for species that are under pres-

431 sure, species that cannot naturally be individually recognised or species that are

432 difficult or dangerous to catch (Thomas & Marques, 2012).

1. ACKNOWLEDGMENTS

REFERENCES

Acevedo, M.A. & Villanueva-Rivera, L.J. (2006) Using automated digital recording systems as effective tools for the monitoring of birds and amphibians. *Wildlife Society Bulletin*, **34**, 211–214.

Ahlen, I. & Baagøe, H.J. (1999) Use of ultrasound detectors for bat studies in europe: experiences from field identification, surveys, and monitoring. *Acta Chiropterologica*, **1**, 137–150.

Anderson, D.R. (2001) The need to get the basics right in wildlife field studies. *Wildlife Society Bulletin*, pp. 1294–1297.

Barlow, J. & Taylor, B. (2005) Estimates of sperm whale abundance in the northeastern temperate pacific from a combined acoustic and visual survey. *Marine Mammal Science*, **21**, 429–445.

Blumstein, D.T., Mennill, D.J., Clemins, P., Girod, L., Yao, K., Patricelli, G., Deppe, J.L., Krakauer, A.H., Clark, C., Cortopassi, K.A. *et al.* (2011) Acoustic monitoring in terrestrial environments using microphone arrays: applications, technological considerations and prospectus. *Journal of Applied Ecology*, **48**, 758–767.

Brusa, A. & Bunker, D.E. (2014) Increasing the precision of canopy closure estimates from hemispherical photography: Blue channel analysis and under-exposure. *Agricultural and Forest Meteorology*, **195**, 102–107.

Buckland, S.T. & Handel, C. (2006) Point-transect surveys for songbirds: robust methodologies. *The Auk*, **123**, 345–357.

Buckland, S.T., Marsden, S.J. & Green, R.E. (2008) Estimating bird abundance: making methods work. *Bird Conservation International*, **18**, S91–S108.

Calisher, C., Childs, J., Field, H., Holmes, K. & Schountz, T. (2006) Bats: important reservoir hosts of emerging viruses. *Clinical microbiology reviews*, **19**, 531–545.

Carbone, C., Cowlishaw, G., Isaac, N.J. & Rowcliffe, J.M. (2005) How far do animals go? Determinants of day range in mammals. *The American Naturalist*, **165**, 290–297.

Clark, C.W. (1995) Application of US Navy underwater hydrophone arrays for scientific research on whales. *Reports of the International Whaling Commission*, **45**,

210–212.

Clement, M.J. & Castleberry, S.B. (2013) Estimating density of a forest-dwelling bat: a predictive model for rafinesque's big-eared bat. *Population Ecology*, **55**, 205–215.

Crespo, E.A., Pedraza, S.N., Grandi, M.F., Dans, S.L. & Garaffo, G.V. (2010) Abundance and distribution of endangered franciscana dolphins in argentine waters and conservation implications. *Marine Mammal Science*, **26**, 17–35.

Cutler, T.L. & Swann, D.E. (1999) Using remote photography in wildlife ecology: a review. *Wildlife Society Bulletin*, pp. 571–581.

Damuth, J. (1981) Population density and body size in mammals. *Nature*, **290**, 699–700.

Depraetere, M., Pavoine, S., Jiguet, F., Gasc, A., Duvail, S. & Sueur, J. (2012) Monitoring animal diversity using acoustic indices: implementation in a temperate woodland. *Ecological Indicators*, **13**, 46–54.

Elphick, C.S. (2008) How you count counts: the importance of methods research in applied ecology. *Journal of Applied Ecology*, **45**, 1313–1320.

Everatt, K.T., Andresen, L. & Somers, M.J. (2014) Trophic scaling and occupancy analysis reveals a lion population limited by top-down anthropogenic pressure in the limpopo national park, mozambique. *PloS one*, **9**, e99389.

Foster, R.J. & Harmsen, B.J. (2012) A critique of density estimation from camera-trap data. *The Journal of Wildlife Management*, **76**, 224–236.

Harris, D., Matias, L., Thomas, L., Harwood, J. & Geissler, W.H. (2013) Applying distance sampling to fin whale calls recorded by single seismic instruments in the northeast atlantic. *The Journal of the Acoustical Society of America*, **134**, 3522–3535.

Hassel-Finnegan, H.M., Borries, C., Larney, E., Umponjan, M. & Koenig, A. (2008) How reliable are density estimates for diurnal primates? *International Journal of Primatology*, **29**, 1175–1187.

Hutchinson, J.M.C. & Waser, P.M. (2007) Use, misuse and extensions of "ideal gas" models of animal encounter. *Biological Reviews of the Cambridge Philosophical Society*, **82**, 335–359.

Jewell, Z. (2013) Effect of monitoring technique on quality of conservation science. *Conservation Biology*, **27**, 501–508.

Jirinec, V., Campos, B.R. & Johnson, M.D. (2011) Roosting behaviour of a migratory songbird on jamaican coffee farms: landscape composition may affect delivery of an ecosystem service. *Bird Conservation International*, **21**, 353–361.

Jones, K.E., Bielby, J., Cardillo, M., Fritz, S.A., O'Dell, J., Orme, C.D.L., Safi, K., Sechrest, W., Boakes, E.H., Carbone, C. *et al.* (2009) PanTHERIA: a species-level database of life history, ecology, and geography of extant and recently extinct mammals: Ecological archives e090-184. *Ecology*, **90**, 2648–2648.

Karanth, K. (1995) Estimating tiger (*Panthera tigris*) populations from camera-trap data using capture–recapture models. *Biological Conservation*, **71**, 333–338.

Kelly, M.J., Betsch, J., Wultsch, C., Mesa, B. & Mills, L.S. (2012) Noninvasive sampling for carnivores. *Carnivore ecology and conservation: a handbook of techniques (L Boitani and RA Powell, eds) Oxford University Press, New York*, pp. 47–69.

Kessel, S., Cooke, S., Heupel, M., Hussey, N., Simpfendorfer, C., Vagle, S. & Fisk, A. (2014) A review of detection range testing in aquatic passive acoustic telemetry studies. *Reviews in Fish Biology and Fisheries*, **24**, 199–218.

Kimura, S., Akamatsu, T., Dong, L., Wang, K., Wang, D., Shibata, Y. & Arai, N. (2014) Acoustic capture-recapture method for towed acoustic surveys of echolocating porpoises. *The Journal of the Acoustical Society of America*, **135**, 3364–3370.

Kunz, T.H., Betke, M., Hristov, N.I. & Vonhof, M. (2009) Methods for assessing colony size, population size, and relative abundance of bats. *Ecological and behavioral methods for the study of bats (TH Kunz and S Parsons, eds) 2nd ed Johns Hopkins University Press, Baltimore, Maryland*, pp. 133–157.

Lammers, M.O. & Au, W.W. (2003) Directionality in the whistles of hawaiian spinner dolphins (stenella longirostris): A signal feature to cue direction of movement? *Marine Mammal Science*, **19**, 249–264.

Lewis, T., Gillespie, D., Lacey, C., Matthews, J., Danbolt, M., Leaper, R., McLanaghan, R. & Moscrop, A. (2007) Sperm whale abundance estimates from acoustic surveys of the ionian sea and straits of sicily in 2003. *Journal of the Marine Biological Association of the United Kingdom*, **87**, 353–357.

526 Manzo, E., Bartolommei, P., Rowcliffe, J.M. & Cozzolino, R. (2012) Estimation of
527   population density of european pine marten in central italy using camera trap-
528   ping. *Acta Theriologica*, **57**, 165–172.

529 Marcoux, M., Auger-Méthé, M., Chmelnitsky, E.G., Ferguson, S.H. & Humphries,
530   M.M. (2011) Local passive acoustic monitoring of narwhal presence in the cana-
531   dian arctic: a pilot project. *Arctic*, pp. 307–316.

532 Marques, T.A., Munger, L., Thomas, L., Wiggins, S. & Hildebrand, J.A. (2011) Es-
533   timating North Pacific right whale (*Eubalaena japonica*) density using passive
534   acoustic cue counting. *Endangered Species Research*, **13**, 163–172.

535 Marques, T.A., Thomas, L., Ward, J., DiMarzio, N. & Tyack, P.L. (2009) Estimating
536   cetacean population density using fixed passive acoustic sensors: An example
537   with Blainville's beaked whales. *The Journal of the Acoustical Society of America*,
538   **125**, 1982–1994.

539 O'Brien, T.G., Kinnaird, M.F. & Wibisono, H.T. (2003) Crouching tigers, hidden
540   prey: Sumatran tiger and prey populations in a tropical forest landscape. *Animal
541   Conservation*, **6**, 131–139.

542 O'Farrell, M.J. & Gannon, W.L. (1999) A comparison of acoustic versus capture
543   techniques for the inventory of bats. *Journal of Mammalogy*, pp. 24–30.

544 Proctor, M., McLellan, B., Boulanger, J., Apps, C., Stenhouse, G., Paetkau, D. &
545   Mowat, G. (2010) Ecological investigations of grizzly bears in canada using dna
546   from hair, 1995-2005: a review of methods and progress. *Ursus*, **21**, 169–188.

547 Purvis, A., Gittleman, J.L., Cowlishaw, G. & Mace, G.M. (2000) Predicting extinc-
548   tion risk in declining species. *Proceedings of the Royal Society of London Series B:
549   Biological Sciences*, **267**, 1947–1952.

550 R Development Core Team (2010) *R: A Language And Environment For Statistical
551   Computing*. R Foundation For Statistical Computing, Vienna, Austria. ISBN 3-
552   900051-07-0.

553 Richter-Dyn, N. & Goel, N.S. (1972) On the extinction of a colonizing species. *The-
554   oretical Population Biology*, **3**, 406–433.

555 Robinson, M. & Stebbings, R. (1997) Home range and habitat use by the serotine
556   bat, eptesicus serotinus, in england. *Journal of Zoology*, **243**, 117–136.

Rogers, T.L., Ciaglia, M.B., Klinck, H. & Southwell, C. (2013) Density can be misleading for low-density species: benefits of passive acoustic monitoring. *Public Library of Science One*, **8**, e52542.

Rovero, F., Zimmermann, F., Berzi, D. & Meek, P. (2013) " which camera trap type and how many do i need?" a review of camera features and study designs for a range of wildlife research applications. *Hystrix*.

Rowcliffe, J.M. & Carbone, C. (2008) Surveys using camera traps: are we looking to a brighter future? *Animal Conservation*, **11**, 185–186.

Rowcliffe, J., Field, J., Turvey, S. & Carbone, C. (2008) Estimating animal density using camera traps without the need for individual recognition. *Journal of Applied Ecology*, **45**, 1228–1236.

Schmidt, B.R. (2003) Count data, detection probabilities, and the demography, dynamics, distribution, and decline of amphibians. *Comptes Rendus Biologies*, **326**, 119–124.

Smouse, P.E., Focardi, S., Moorcroft, P.R., Kie, J.G., Forester, J.D. & Morales, J.M. (2010) Stochastic modelling of animal movement. *Philosophical Transactions of the Royal Society B: Biological Sciences*, **365**, 2201–2211.

Soisalo, M.K. & Cavalcanti, S. (2006) Estimating the density of a jaguar population in the Brazilian Pantanal using camera-traps and capture-recapture sampling in combination with GPS radio-telemetry. *Biological Conservation*, **129**, 487–496.

Sollmann, R., Gardner, B., Chandler, R.B., Shindle, D.B., Onorato, D.P., Royle, J.A. & O'Connell, A.F. (2013) Using multiple data sources provides density estimates for endangered florida panther. *Journal of Applied Ecology*, **50**, 961–968.

SymPy Development Team (2014) *SymPy: Python library for symbolic mathematics.*

Thomas, L. & Marques, T.A. (2012) Passive acoustic monitoring for estimating animal density. *Acoustics Today*, **8**, 35–44.

Trolle, M. & Kéry, M. (2003) Estimation of ocelot density in the Pantanal using capture-recapture analysis of camera-trapping data. *Journal of mammalogy*, **84**, 607–614.

Trolle, M., Noss, A.J., Lima, E.D.S. & Dalponte, J.C. (2007) Camera-trap studies of maned wolf density in the Cerrado and the Pantanal of Brazil. *Biodiversity and Conservation*, **16**, 1197–1204.

589 Wright, S.J. & Hubbell, S.P. (1983) Stochastic extinction and reserve size: a focal
590   species approach. *Oikos*, pp. 466–476.

591 Yapp, W. (1956) The theory of line transects. *Bird study*, **3**, 93–104.

592 Zero, V.H., Sundaresan, S.R., O'Brien, T.G. & Kinnaird, M.F. (2013) Monitoring
593   an endangered savannah ungulate, Grevy's zebra (*Equus grevyi*): choosing a
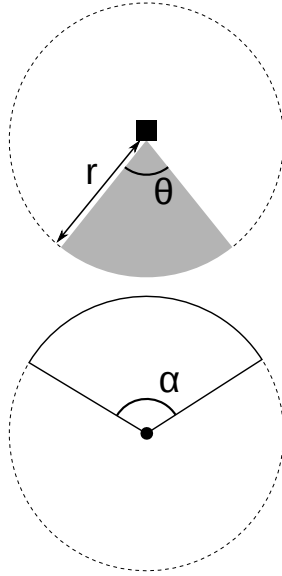594   method for estimating population densities. *Oryx*, **47**, 410–419.

FIGURE 1. Representation of sensor detection width and animal signal width. The filled square and circle represent a sensor and an animal, respectively; θ, sensor detection width (radians); r, sensor detection distance; dark grey shaded area, sensor detection zone; α, animal signal width (radians). Dashed lines around the filled square and circle represents the maximum extent of θ and α, respectively.
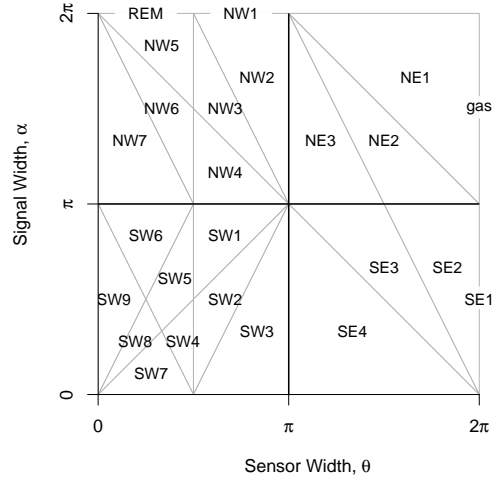
FIGURE 2. Locations where derivation of the average profile $\bar{p}$ is the same for different combinations of sensor detection width and animal signal width. Symbols within each polygon refer to each gREM submodel named after their compass point, except for Gas and REM which highlight the position of these previously derived models within the gREM. Symbols on the edge of the plot are for submodels with $\alpha, \theta = 2\pi$
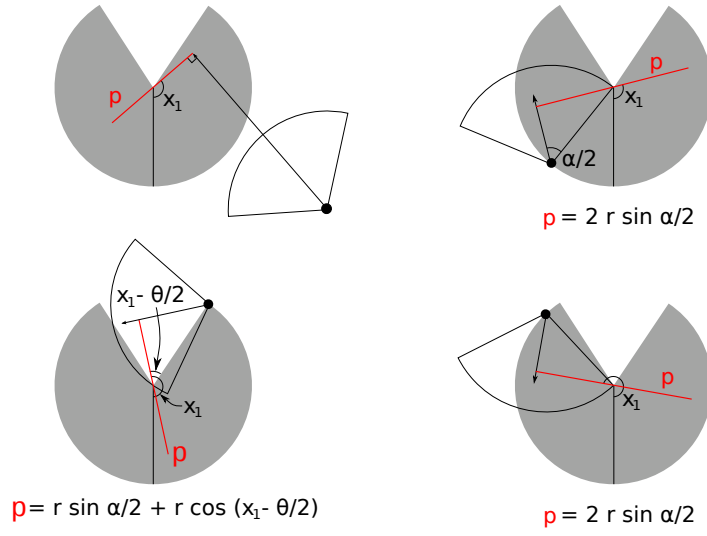
FIGURE 3. An overview of the derivation of SE2. The filled circles represent animals, with the animal signal shown as a unfilled sector and the direction of movement shown as an arrow. The detection zone of the sensors are shown as filled grey sectors with a detection distance of r. The SYMBOL shows the direction the sensor is facing; θ, sensor detection width; α, animal signal width. The profile p (the line an animal must pass through in order to be captured) is shown in red and x_1 is the focal angle, where (a) shows the location of x_1. The derivation of p changes as the animal approaches the sensor from different directions where (b) is the derivation of p when x_1 is in the interval $[\frac{\pi}{2}, \frac{\pi}{2} + \frac{\theta}{2} - \frac{\alpha}{2}]$, (c) p when x_1 is in the interval $[\frac{\pi}{2} + \frac{\theta}{2} - \frac{\alpha}{2}, \frac{5\pi}{2} - \frac{\theta}{2} - \frac{\alpha}{2}]$ and (d) p when x_1 is in the interval $[\frac{5\pi}{2} - \frac{\theta}{2} - \frac{\alpha}{2}, \frac{3\pi}{2}]$. The resultant equation for p is shown beneath each figure.
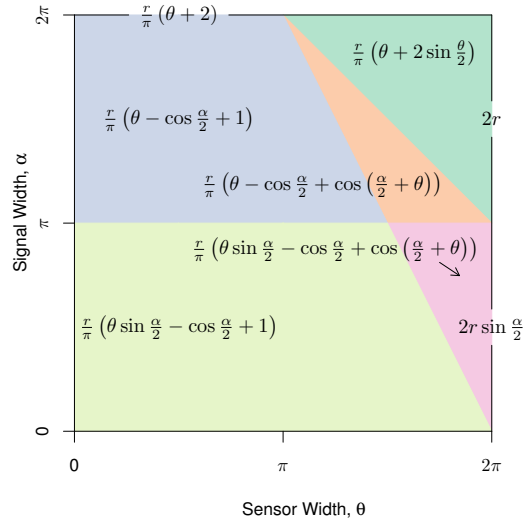
FIGURE 4. Expressions for the average profile width, $\bar{p}$, given sensor and signal widths. Despite independent derivation within each block, many models result in the same expression. These are collected together and presented as one block of colour. Expressions on the edge of the plot are for submodels with $\alpha, \theta = 2\pi$.
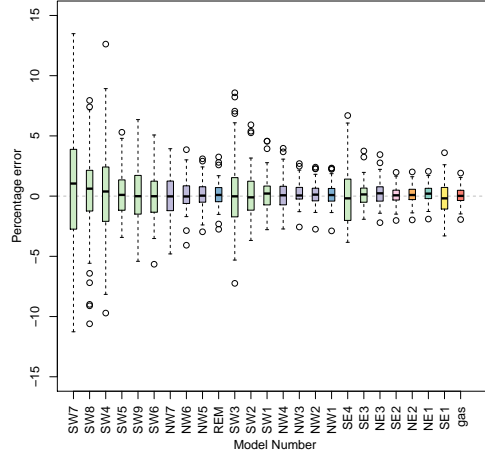
FIGURE 5. Simulation model results of the accuracy and precision for gREM submodels. The precentage error between estimated and true density for each gREM sub model is shown within each box plot, where the black line represents the median percentage error across all simulations, boxes represent the the middle 50% of the data. Box colours correspond to the expressions for average profile width $\bar{p}$ given in Figure 4.
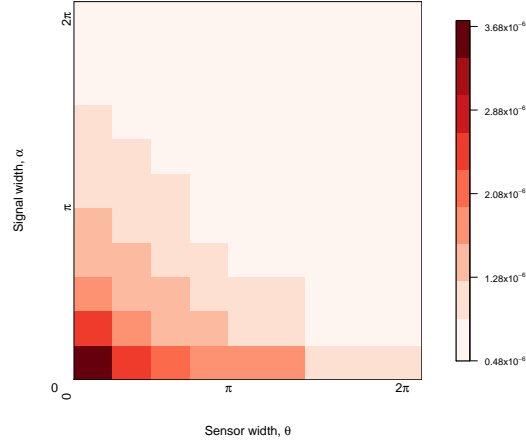
FIGURE 6. Simulation model results of the gREM precision given a range of sensor and signal widths, shown by the standard deviation of the error between the estimated and true densities. Standard deviations are shown from deep red to pink, representing high to low values between 0.483×10^{-6} to 3.74×10^{-6}.
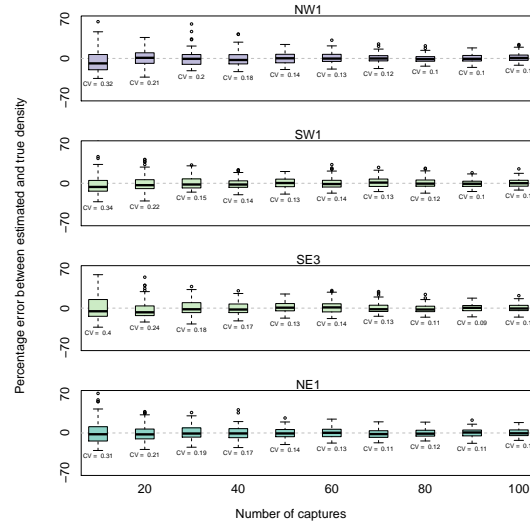
FIGURE 7. Simulation model results of the accuracy and precision of four gREM submodels (NW1, SW1, SE3 and NE1) given different numbers of captures. The percentage error between estimated and true density within each gREM sub model for capture rate is shown within each box plot. Sensor and signal widths vary between submodels. The colour of each box plot corresponds to the expressions for average profile width $\bar{p}$ given in Figure 4.
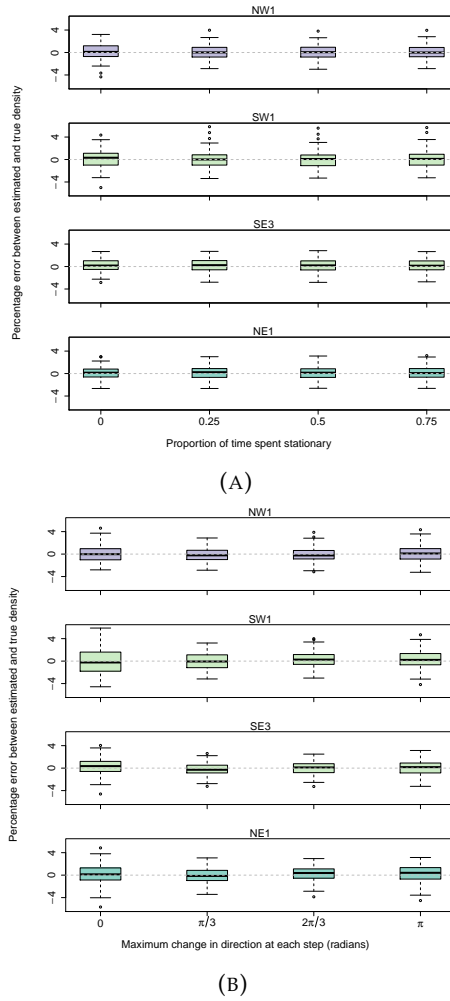
(A)

(B)

FIGURE 8. Simulation model results of the accuracy and precision of four gREM submodels (NW1, SW1, SE3 and NE1) given different movement models where (A) amount of time spent stationary (stop-start movement) and (B) maximum change in direction at each step (correlated random walk model). The percentage error between estimated and true density within each gREM sub model for the different movement models is shown within each box plot. The simple model is represented where time and maximum change in direction equals 0. The colour of each box plot corresponds to the expressions for average profile width $\bar{p}$ given in Figure 4.